

with the theoretical predictions. The ${}^2F_{7/2}$ and ${}^2F_{5/2}$ states are found to have similar properties and have large reduced widths for the He³+He⁴ configuration and small reduced widths for the p +Li⁶ configuration.

It is worthwhile to consider some of the questions that still need to be answered with regard to the level structure of Li⁷ and Be⁷.

(1) The separation of the 2F states is calculated by most nuclear models to be about 1 MeV, while the observed separation is closer to 2 MeV. Shell-model calculations have indicated¹² that this discrepancy may be removed by allowing configuration mixing. Is it possible to allow sufficient mixing to fit the observed energy separation, while keeping small the ratio of the reduced width for the p +Li⁶ configuration to that of the He³+He⁴ configuration? In connection with this point, does the fact that the two 5/2⁻ levels overlap strongly in energy but do not appear to mix appreciably indicate

the presence of other "quantum numbers" which allow these states to remain almost orthogonal?

(2) These data together with the Li⁶(p,p)Li⁶ data of Whitehead indicate that above the ${}^4P_{5/2}$ level only one additional level is clearly visible below an excitation energy of 14 MeV. How can this be reconciled with the theoretical predictions that there should be a large number of possible levels in this energy range?

ACKNOWLEDGMENTS

The authors wish to acknowledge fellowship aid from the National Science Foundation during the course of this work. We also wish to thank Professor T. Lauritsen, Professor C. A. Barnes, and A. D. Bacher for their help in taking the data, and Mrs. Barbara Hinds and D. Papanastassiou for help with the data reduction. The help given by Dr. A. C. L. Barnard in allowing us to see the Rice data and phase-shift analysis prior to publication is greatly appreciated.

Emission of Li³, Be, and B Fragments from Nuclei in Photographic Emulsion

F. O. BREIVIK, T. JACOBSEN, AND S. O. SØRENSEN

Institute of Physics, University of Oslo, Oslo, Norway

(Received 6 September 1962)

A method of identification of tracks of heavy fragments emitted from highly excited nuclei in photographic emulsions exposed to 4.5-GeV negative pions is described. Charge spectra, energy spectra, angular distributions, etc., of the fragments are determined. An argument is presented for an isotropic emission of the fragments in the system of the moving parent Ag—or Br—nucleus.

INTRODUCTION

DURING the last few years extensive investigations of the emission of heavy fragments from high-energy nuclear disintegrations have been undertaken by various laboratories.¹⁻²¹

The present paper deals with observations of lithium, beryllium, and boron fragments emitted from nuclear disintegrations produced by 4.5-GeV negative pions from the Berkeley Bevatron. The events were recorded in a stack of 200 stripped, electron sensitive Ilford G5 emulsions, each 10×15 cm and 600 μ thick. The pion beam entered the stack perpendicular to the 15-cm edge, and parallel to the plane of the emulsion, the intensity varying between 10⁶–10⁸ cm⁻² perpendicular to the direction of the beam.

- ¹ A. Bonetti and C. Dilworth, *Phil. Mag.* **40**, 585 (1949).
- ² P. Hodgson and D. H. Perkins, *Nature* **163**, 439 (1949).
- ³ D. H. Perkins, *Proc. Roy. Soc. (London)* **A203**, 399 (1950).
- ⁴ B. A. Munir, *Phil. Mag.* **1**, 355 (1956).
- ⁵ S. J. Goldsack, W. O. Lock, and B. A. Munir, *Phil. Mag.* **2**, 149 (1957).
- ⁶ S. Nakagawa, E. Tamai, H. Huzita, and K. Okudaira, *J. Phys. Soc. Japan* **12**, 747 (1957).
- ⁷ O. V. Lozhkin and N. A. Perfilov, *Zh. Eksperim. i Teor. Fiz.* **31**, 913 (1956) [translation: *Soviet Phys.—JETP* **4**, 790 (1957)].
- ⁸ E. Baker and S. Katcoff, *Bull. Am. Phys. Soc.* **2**, 222 (1957).
- ⁹ V. I. Ostrumov, *Zh. Eksperim. i Teor. Fiz.* **32**, 3 (1957) [translation: *Soviet Phys.—JETP* **5**, 12 (1957)].
- ¹⁰ O. V. Lozhkin, *Zh. Eksperim. i Teor. Fiz.* **33**, 354 (1957) [translation: *Soviet Phys.—JETP* **6**, 273 (1958)].
- ¹¹ E. Tamai, *Nuovo Cimento*, **14**, 1 (1958).
- ¹² V. P. Shamov, *Zh. Eksperim. i Teor. Fiz.* **35**, 316 (1958) [translation: *Soviet Phys.—JETP* **8**, 219 (1958)].
- ¹³ S. Katcoff, *Phys. Rev.* **114**, 905 (1959).
- ¹⁴ O. Skjeggstad and S. O. Sørensen, *Phys. Rev.* **113**, 1115 (1959).

- ¹⁵ O. Skjeggstad, *Arch. Math. Natur.* **B54**, No. 7 (1959).
- ¹⁶ K. Imaeda, M. Kazuno, and N. Ito, *J. Phys. Soc. (Japan)* **15**, 1753 (1960).
- ¹⁷ E. W. Baker, S. Katcoff, and C. P. Baker, *Phys. Rev.* **117**, 1352 (1960).
- ¹⁸ U. R. Arifkhanov, M. M. Makarov, N. A. Perfilov, and V. P. Shamov, *Zh. Eksperim. i Teor. Fiz.* **38**, 1115 (1960) [translation: *Soviet Phys.—JETP* **11**, 806 (1960)].
- ¹⁹ O. V. Lozhkin, N. A. Perfilov, A. A. Rimskii-Korsakov and J. Fremlin, *Zh. Eksperim. i Teor. Fiz.* **38**, 1388 (1960) [translation: *Soviet Phys.—JETP* **11**, 1001 (1960)].
- ²⁰ E. W. Baker and S. Katcoff, *Phys. Rev.* **123**, 641 (1961).
- ²¹ W. Gajewaki, J. Pniewski, T. Pniewski, J. Siemińska, M. Soltan, K. Soltyński, and J. Suchorzewska, Report No. 286/VI Polish Acad. of Sciences (1961).

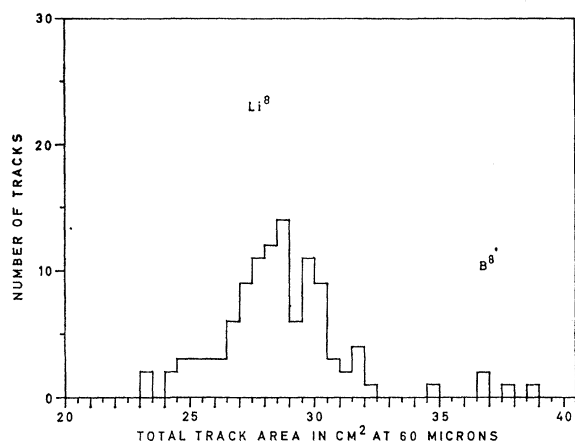


FIG. 1. Histogram showing the projected total track area of the last 60μ of hammer tracks.

In part I we describe a new photographic method for determining the charge of particles in nuclear emulsions. It is based on an improvement of the identification method developed in earlier experiments.

In Parts II-IV the observed energy spectra, angular distributions, etc., of the Li^8 , beryllium, and boron fragments are presented.

I. CHARGE DETERMINATION

Skjeggstad²² has described a method for charge determination of heavy fragments in electron-sensitive nuclear emulsions. The identification of the fragments was based on measurements of track areas, attention being confined to tracks dipping at angles $< 20^\circ$ to the plane of the emulsion. The areas were determined from

the track profile projected onto a screen. Drawings of the tracks were subdivided into short cells, and the area of each cell was measured with a high-precision planimeter. By integrating the areas of the cells over a certain track length it was shown that the tracks were clearly separated into groups corresponding to different charge values.

Using a projecting microscope the magnification obtainable is strongly limited by the low intensity of the visible light from the microscope bulb relative to its thermal radiation, since too much absorption in the photographic plate destroys the emulsion. In order to avoid this limiting effect the following improvement of the previous method was developed:

With a $\times 97$ microscope objective and a $\times 8$ ocular, a series of microphotographs of the tracks was taken, using a Leica camera and Kodak Micro-File film. We adopted the convention that at least 10μ of the track should be in focus on each microphotograph. This confined the measurements to tracks with an angle of dip $< 15^\circ$ in the developed emulsion. By means of an ordinary Leitz projector and a reflecting mirror, a picture of the tracks was projected onto a horizontal screen, and a drawing of the contours of the fragment was made on tracing paper. It was found convenient to work with a magnification of ~ 8000 . The rest of the analysis was analogous with Skjeggstad's method. We believe that the introduction of this photographic link in the determination of charge by track-area measurements represents a considerable improvement.

In order to investigate the potentialities and the resolution power of the method, a series of measurements was performed on tracks of known identity.

In Fig. 1, track-area measurements on "hammer

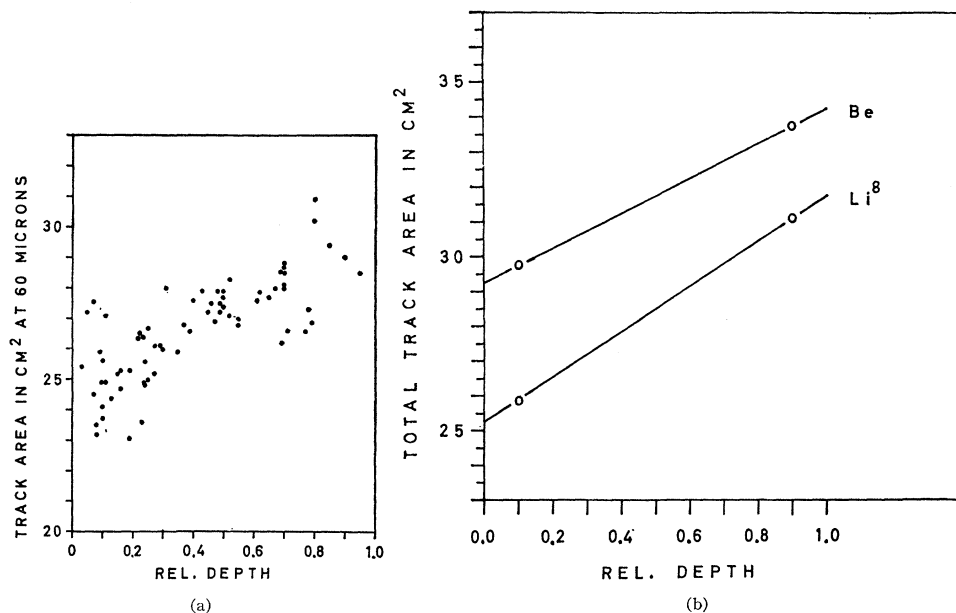


FIG. 2. (a) Variation of the projected 60μ residual track area with the depth in the emulsion. (b) Variation in the projected track area of a Li^8 and a Be^8 track by microphotographing the tracks from both sides of the stripped emulsion.

²² O. Skjeggstad, Arch. Math. Natur. **B54**, No. 1 (1956).

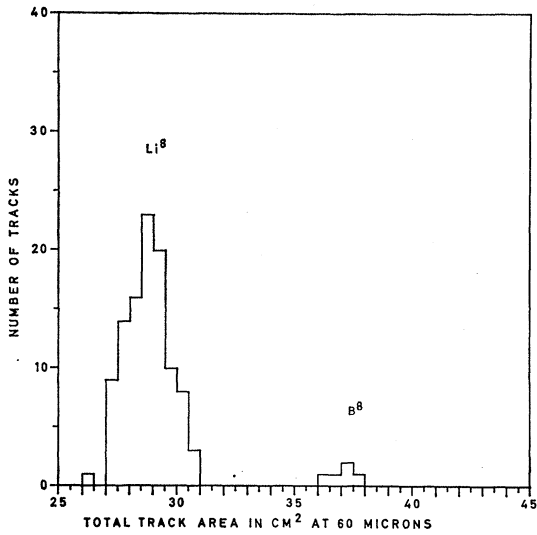


FIG. 3. Histogram showing the projected total track area of the last 60μ of hammer tracks, corrected for depth in the emulsions and illumination conditions.

tracks" emitted from stars are shown. The figure reveals two groups of tracks, corresponding to Li^8 and B^8 , respectively. Apart from the statistical fluctuations in the ionization produced by the fragments, the two main effects which tend to broaden the track area distributions are: (1) variation in the area of a photographed track with the depth in the emulsion; (2) variation in the area with the exposure time and the illumination conditions.

In order to study the variation in the track area of identical particles with the depth in the emulsion, the track area of the last 60μ of 72 Li^8 nuclei was plotted

against its depth in the emulsion. The result is shown in Fig. 2(a). It indicates an increase of 20% in the track area from the top of the emulsion to the bottom. This effect does not reflect a real gradient variation in the average width of a track due to the processing of the

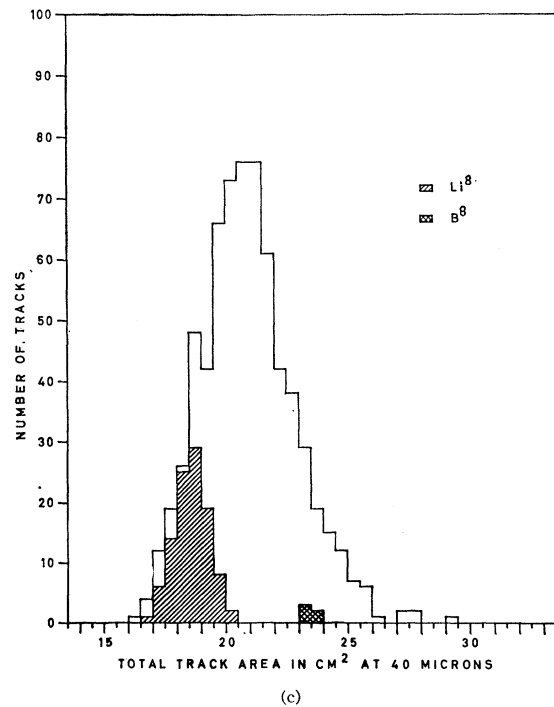
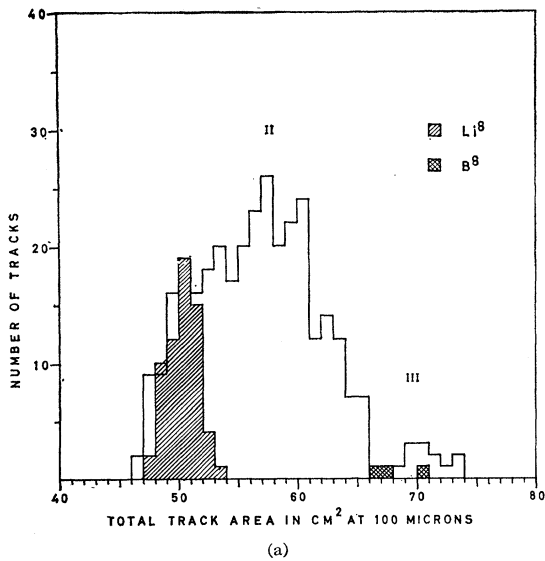
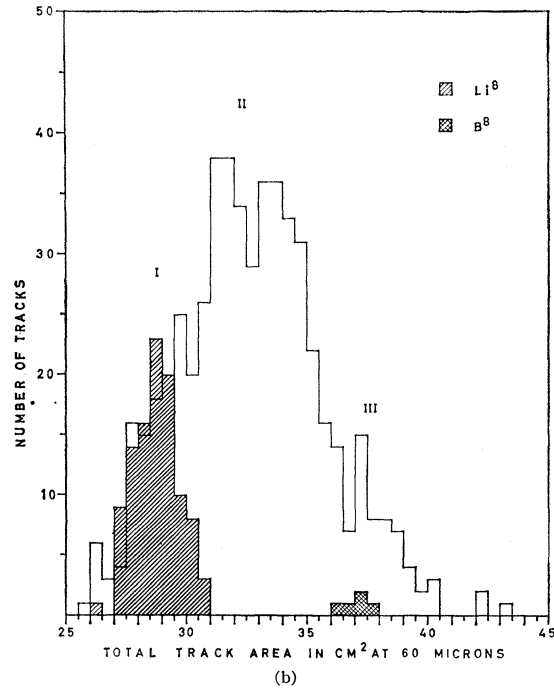


FIG. 4. Histograms, corrected for depth and illumination, showing the projected total track area of residual range of (a) 100μ (328 tracks), (b) 60μ (358 tracks), (c) 40μ (678 tracks), of heavy nuclear fragments. The shaded histograms represent the measurements on hammer tracks superposed.

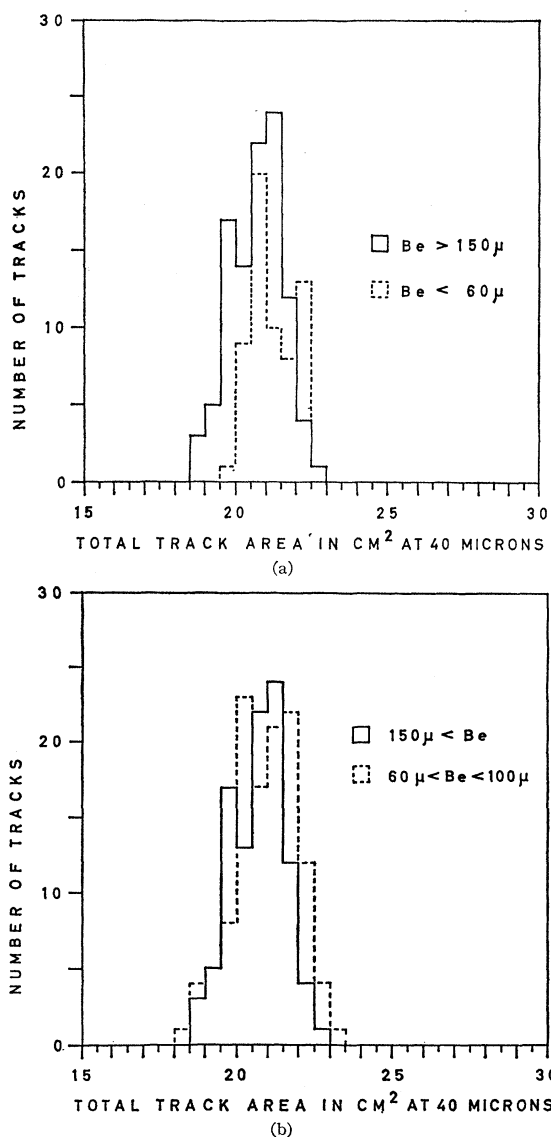


FIG. 5. The projected total track area of the last 40 μ of beryllium tracks of (a) range $R < 60 \mu$ and $R > 150 \mu$, respectively; (b) range $60 \mu < R < 100 \mu$ and $R > 150 \mu$, respectively.

emulsion, but an optical effect, making the contours of the deeper laying tracks more diffuse on microphotographs. This is proved by stripping some emulsions from the glass and microphotographing tracks from two opposite sides of the emulsion. Two typical examples are shown in Fig. 2(b).

If the real area of a track is A_0 , Figs. 2(a) and 2(b) show that the observed track area A_{obs} is approximately given by formula

$$A_{\text{obs}} = A_0(1 + kD), \quad (1)$$

where D is the depth of the track from the surface of the emulsion and k is a constant. When applying formula (1) for depth corrections, we have used the same value of k for both types of fragments.

The emulsions were very inhomogeneously exposed to the pion beam, and the light transparency of the emulsions varies strongly from plate to plate. Further, the area of a photographed track varies markedly with the amount of exposure of light. We have tried to work out correction factors for these effects, by referring all the track area measurements to a standard light transparency of the microfilms.

In Fig. 3 is shown the A_0 values of the hammer tracks in Fig. 1, calculated from (1), and corrected for variation in the illumination conditions. An increase in the discrimination between Li^8 and B^8 is immediately apparent.

Figures 4(a), (b), and (c) show the results of area measurements made on tracks of fragments emitted from stars. The area measurements have been corrected for the depth of the track in the emulsion and the illumination conditions. The criteria for the selection of the tracks were as follows: (1) The tracks ended in the emulsion. (2) They appeared by visual inspection to have charge $Z > 3$. (3) The ranges were $> 40 \mu$. (4) The tracks were located between 50μ and 550μ from the surface of the emulsion. (5) Only fragments from stars with a number of heavily ionizing prongs $N_h \geq 7$ were considered.

The shaded area represents the measurements on hammer tracks. It is evident from Fig. 4 that the majority of the tracks represents beryllium fragments with two "tails" due to stable lithium and boron fragments, respectively. This attribution is based on the fact that the two "tails" I and III appear to coincide with the histograms of the hammer tracks Li^8 and B^8 , respectively. The presence of lithium in the charge spectrum results from the effect that a scanner selecting tracks according to the criteria (1)–(5) sometimes overestimates the charge of a fragment. The relatively large proportion of lithium nuclei in the charge spectrum Fig. 4(a) indicates that the loss of fragments with $Z > 3$ and range $> 100 \mu$ during scanning is negligible.

On the basis of the diagrams 4(a)–(c), a fragment was defined as beryllium or boron according to this convention:

	Residual range	Beryllium	Boron
Fig. 4(a)	100 μ	(54–64) cm^2	(66–74) cm^2
Fig. 4(b)	60 μ	(31–35.5) cm^2	(36.5–40.5) cm^2
Fig. 4(c)	40 μ	(20–22.5) cm^2	(23.0–25.0) cm^2

Obviously, this method of selecting fragments is somewhat arbitrary. The "beryllium" group will contain lithium and boron, and the "boron" group beryllium and possibly a small admixture of nuclei of charge $Z > 5$. It is reasonable to assume that these contaminations are relatively small. In the following this method of selecting fragments will, therefore, be considered as a sufficient approximation.

II. THE EXPERIMENTAL ENERGY SPECTRA

The classification of the heavy fragments in the present investigation is exclusively based on the above method of charge identification. Therefore, when presenting the observed energy spectra, the question arises as to whether or not the method has any bias in selecting tracks of different range. In a previous investigation¹⁴ the effect of losing short tracks during the scanning was discussed in connection with the energy spectra of Li^6 and Li^7 nuclei. In the present experiment, however, we assume this effect to be less important due to the very heavy ionization of particles with charge $Z > 3$. A strong argument in favor of this is given by the large proportion of lithium nuclei observed in the charge spectra, Fig. 4.

Still, it is reasonable to assume a certain loss of short beryllium tracks compared to boron. In order to investigate this effect the beryllium tracks were divided into two groups of ranges $R < 60 \mu$ and $R > 150 \mu$, respectively. The distribution of the total track area of the last 40μ of the two groups is shown in Fig. 5(a). It is immediately apparent that the last 40μ of the shorter tracks are more heavily ionizing than those of the longer tracks. A possible explanation of this effect is that some shorter beryllium tracks (range $< 60 \mu$) of smaller track width are lost during scanning and by the procedure of

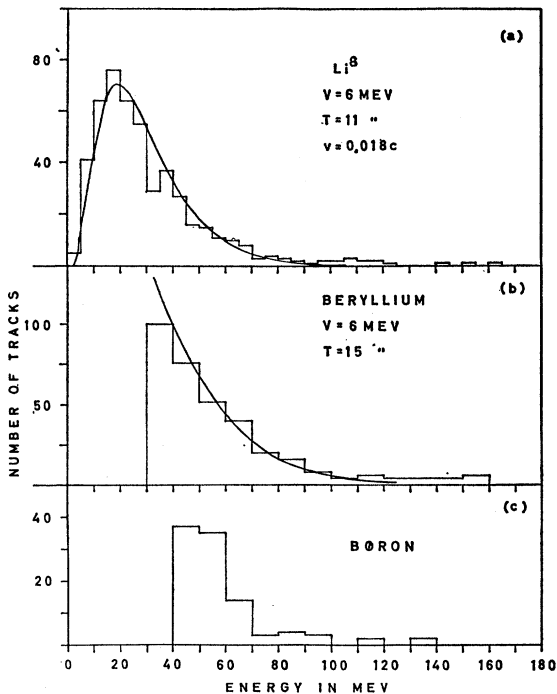
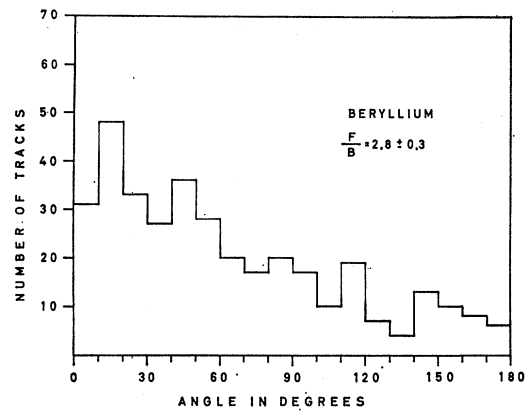
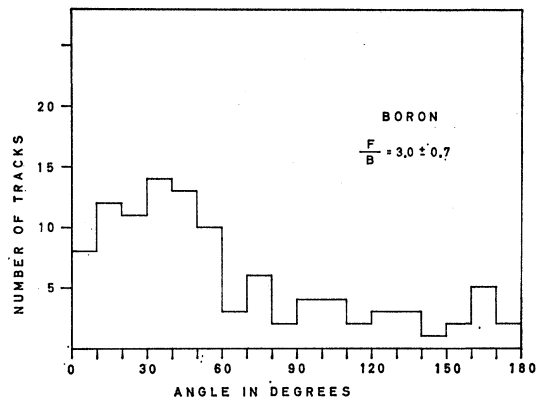


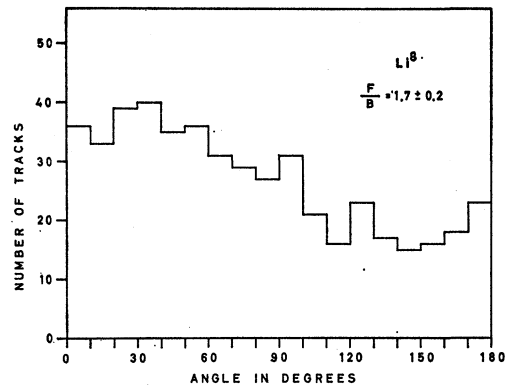
FIG. 6. The experimental energy spectrum of (a) 483 Li^8 hammer tracks with dip angle $< 15^\circ$; (b) 259 beryllium fragments; (c) 106 boron fragments. The curves are calculated from Weisskopf evaporation formula (reference 26) assuming a potential barrier $V = 6 \text{ MeV}$ and $T = 11 \text{ MeV}$ for Li^8 and $V = 6 \text{ MeV}$ and $T = 15 \text{ MeV}$ for beryllium. The curve (a) is corrected for a velocity $v = 0.018c$ of the evaporating nucleus (reference 14).



(a)



(b)



(c)

FIG. 7. Angular distribution of (a) Be fragments of range $R > 40 \mu$; (b) B fragments of range $R > 40 \mu$; (c) Li^8 fragments. F/B give the forward/backward ratio.

selecting beryllium fragments from Fig. 4. Also a contamination of boron in the group of short beryllium tracks is possible. In Fig. 5(b) a similar plot for beryllium tracks of ranges $60 \mu < R < 100 \mu$ and $R > 150 \mu$ is shown. Here these effects are less pronounced. Therefore, our energy spectrum of beryllium may be regarded as reliable for $R > 60 \mu$, corresponding to kinetic energy $> 34 \text{ MeV}$. The high-energy portion of the spectrum

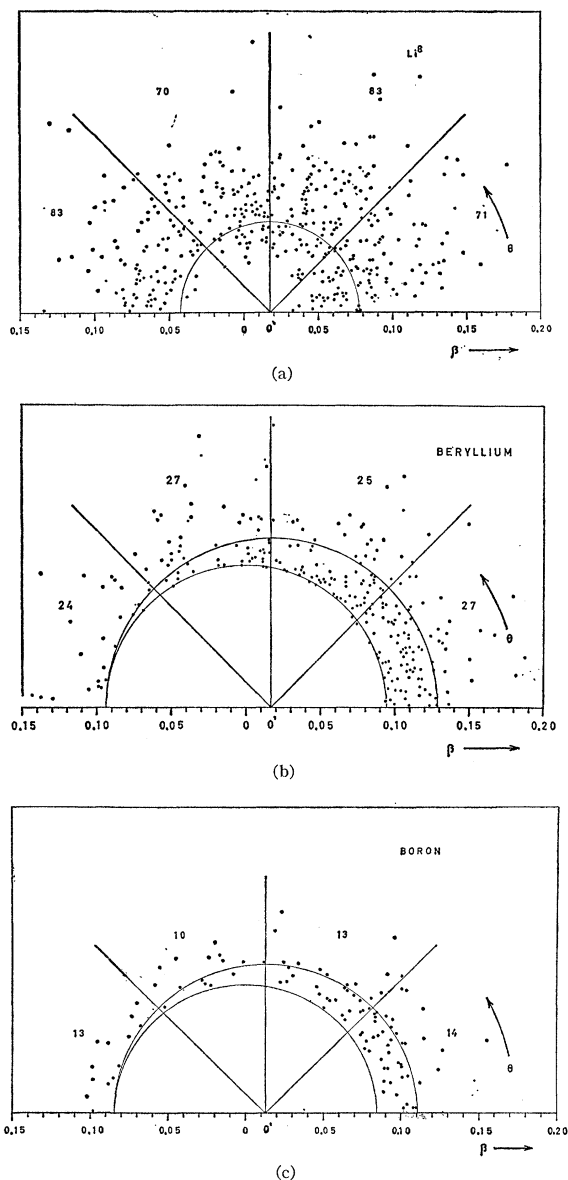


FIG. 8. Polar-coordinate plot showing velocity $\beta=v/c$ and projected angle θ for (a) Li^8 giving $OO' \sim 0.018$; (b) Be giving $OO' \sim 0.016$; (c) B giving $OO' \sim 0.013$.

is reliable to the same extent as the identification of long-range tracks based on Fig. 4(a).

In Figs. 6(b) and (c) the energy spectra of 259 beryllium and 106 boron fragments, respectively, are plotted. In calculating these spectra we have assumed the two types of nuclei to be isotopes of Be^9 and B^{11} , respectively. In Fig. 6(a) the energy spectrum of 483 Li^8 fragments out of a total material of 1167 observed in the present experiment is shown. The reduction has been made to reduce geometrical loss factors, and, therefore, only tracks with an angle of dip $< 15^\circ$ were considered.

Because of the characteristic "hammer shape" at the

end of a Li^8 track, these tracks are easy to find during scanning. Therefore, scanning loss will not be so important as for Be and B. We have used the empirical range-energy relations of Barkas²³ for heavy ions.

III. THE EXPERIMENTAL ANGULAR DISTRIBUTIONS

The angles of emission of the fragments have been measured with respect to the direction of motion of the incoming pions. In Figs. 7(a) and (b) the angular distributions of the beryllium and boron nuclei of range $> 40 \mu$ are shown. In Fig. 7(c) the angular distribution for Li^8 nuclei is shown. All types of fragments are seen to be characterized by a strong forward collimation.

This presentation of the angular distributions does not, however, decide the important question of whether the emission of the fragments is an isotropic or anisotropic process in the system of the moving parent Ag or Br nucleus.

In the following this moving frame of reference will be called the "emission system" (E.S.). The problem then arises as to whether the observed forward collimation of the fragments has to be explained by a cascade process or by an isotropic emission from a moving E.S. Although this question is very difficult to investigate, an argument will be presented for the existence of a frame of reference in which the majority of the fragments are emitted isotropically.

In Figs. 8(a), (b), and (c) are shown polar diagrams of the velocities $\beta=v/c$ and angles of emission θ in the laboratory system of the Li^8 , beryllium, and boron fragments observed in the present experiment. To avoid loss effects, only Li^8 tracks of dip $< 10^\circ$ and beryllium and boron tracks $< 15^\circ$ are considered. In the case of beryllium and boron, only velocities $\beta > 0.094$ and $\beta > 0.085$, respectively, are considered due to the applied method of charge determination. It is seen from the beryllium and boron diagrams that a circle can be drawn around points O' on the polar axis, outside which approximately equal numbers of (β, θ) points are contained in equal angular intervals. Further, the velocity spectra in each of the angular sectors are very similar, indicating that direct "knock-on" or cascade processes are negligible. This suggests that the distance OO' could measure the average velocity of the E.S. in the laboratory system. This is given additional support by the fact that $OO' \sim 0.01-0.02$, which is of the same order of magnitude as the velocities of the recoil nuclei in high-energy nuclear interactions.^{24,25} Although not conclusive, these indications show that the observations are consistent with an isotropic emission of the beryllium and boron fragments in an E.S.

The Li^8 material in Fig. 8(a) has no 40μ cutoff and is, therefore, of particular interest. It is seen that isotropy may be obtained for the high-energy Li^8 for $OO' \sim 0.018$, but then the low-energy Li^8 will be anisot-

²³ W. H. Barkas, Phys. Rev. **89**, 1019 (1953).

²⁴ J. B. Harding, Phil. Mag. **40**, 530 (1949).

²⁵ N. Porile, Phys. Rev. **120**, 572 (1960).

ropically distributed. This anisotropy of the low-energy fragments may be explained as a loss effect in the following way: Assume the low-energy fragments to be emitted isotropically in the E.S., and the velocity of the E.S. to be of the same order of magnitude as the velocities of the low-energy Li^8 fragments. The fragments going backward in the E.S. will then obtain very small velocities in the laboratory system. These fragments should, therefore, be observed in the emulsion as tracks with ranges of only a few microns, and would most probably be impossible to detect during scanning. Therefore we may conclude that the emission of all the Li^8 fragments presumably is isotropic in the E.S.

IV. FRAGMENT PRODUCTION AND NUCLEAR EXCITATION

In order to study the mechanism of ejection of heavy fragments, the energy spectra and relative frequencies of the fragments have to be compared with the energy released in the nuclear disintegrations. As a measure of the latter we use the number of heavily ionizing prongs N_h , defined as the number of tracks with grain density greater than 1.4 times minimum.

In Figs. 9(a), (b), and (c) the values of the kinetic energy of Li^8 , Be , and B fragments and the corresponding value of N_h are plotted. As will be seen in the figures, no strong correlation exists between the particular energy with which a heavy fragment is emitted and the energy release of the associated nuclear disintegration.

Due to uncertainties in the identification method described above, the absolute values of the boron/beryllium ratio cannot be determined with precision in the present experiment. The general trend in the variation of this ratio may, however, be investigated.

In Fig. 10 the distributions in N_h for stars emitting beryllium and boron fragments of range $>40 \mu$ and Li^8 are shown. The observations indicate a slight increase in the average value of N_h with the charge of the fragment. This is in agreement with previous experiments.¹⁵ Another demonstration of this effect is given in Fig. 11 which shows the total track area in the last 60μ of the fragments in Fig. 4(b) for $N_h > 18$ and $N_h \leq 18$. The figure clearly illustrates the larger proportion of heavily ionizing tracks in the bigger stars.

On the basis of Fig. 11 we have calculated the beryllium/boron ratio to be 3.6 ± 0.7 and 9.4 ± 2.4 for $N_h > 18$ and $N_h \leq 18$, respectively, for tracks of range $>60 \mu$.

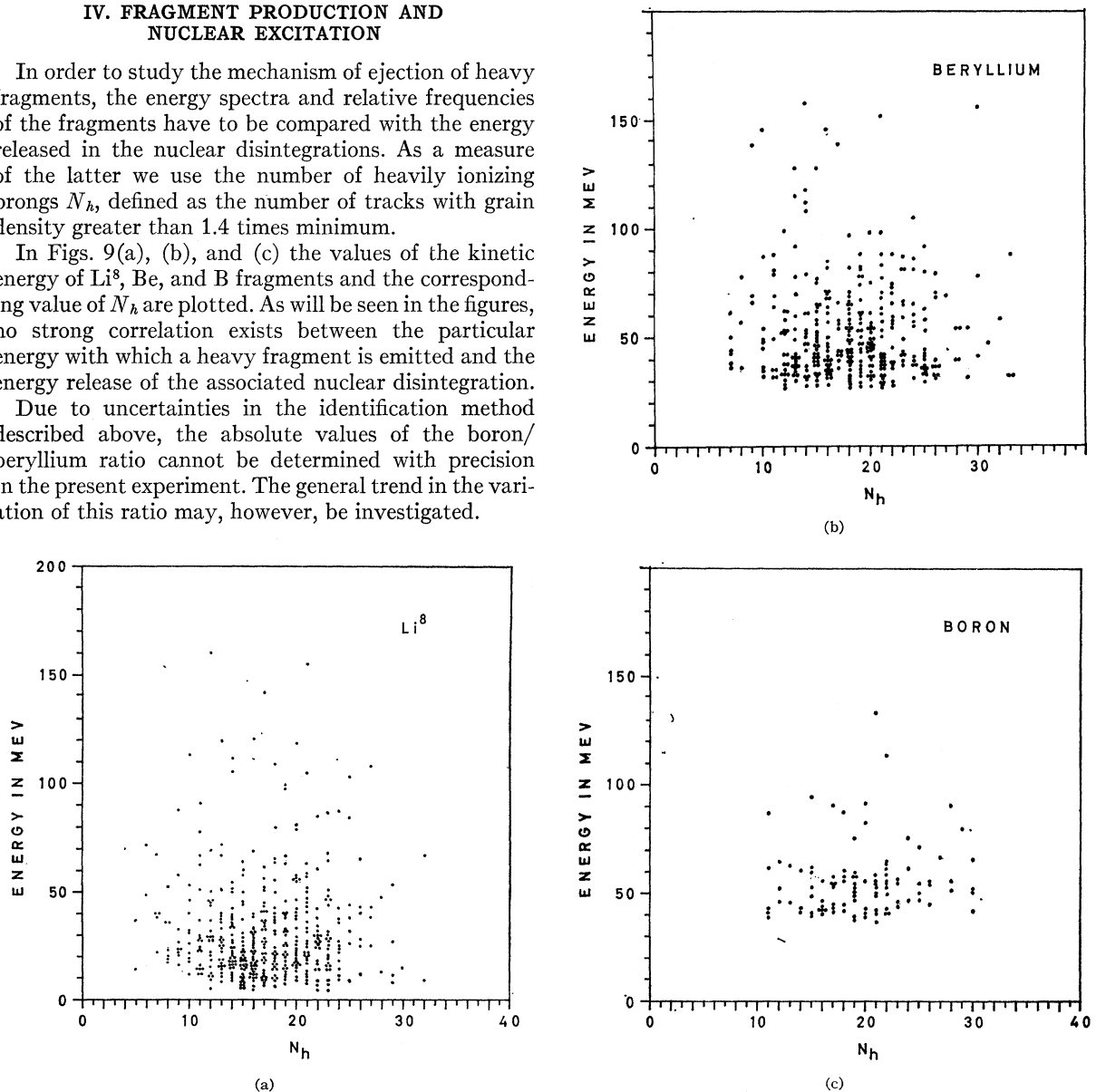


FIG. 9. Kinetic energy of (a) Li^8 , (b) Be , and (c) B fragments plotted vs corresponding number N_h of heavily ionizing prongs.

V. DISCUSSION

In a previous paper¹⁴ the experimental data on the energy spectra, angular distributions, relative frequencies, etc., of heavy fragments ejected from stars were compared with the predictions from the nuclear evaporation theory. In particular the observations of Li^8 nuclei were subjected to a detailed analysis. The conclusion drawn from these discussions was that the majority of the Li^8 nuclei could not be emitted in a nuclear evaporation process. The main reason for this conclusion was the very broad energy spectrum of the ejected fragments, corresponding to mean nuclear temperatures ~ 11 MeV.

The energy spectra, Figs. 6(a), (b), and (c), also indicate high nuclear temperatures. The present identification method does not allow the observation of the maxima in the energy spectra of the beryllium and the boron fragments. The slight slope of the spectra, however, can only be interpreted on the basis of evaporation theory²⁶

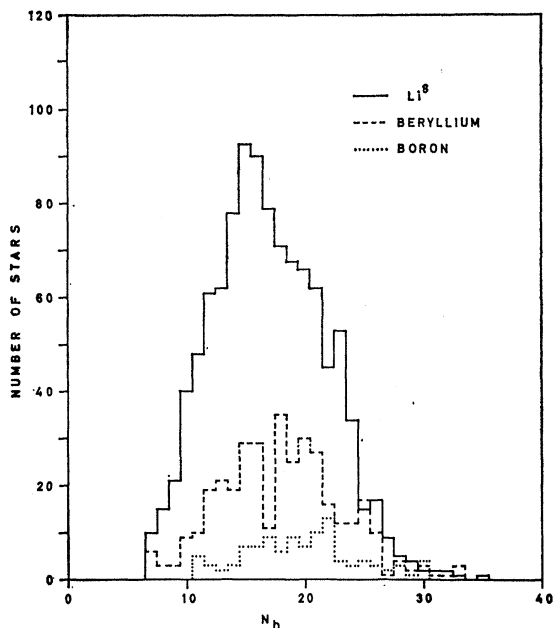


FIG. 10. Histograms showing the distributions of N_h for stars emitting beryllium and boron fragments of range $R > 40 \mu$ and Li^8 .

²⁶ V. Weisskopf, Phys. Rev. **52**, 295 (1937).

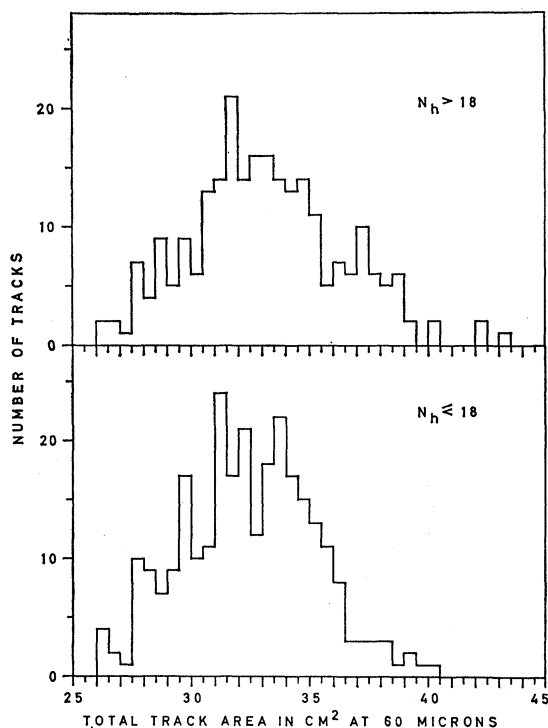


FIG. 11. Total track area of the last 60μ of the fragments for $N_h > 18$ and $N_h \leq 18$.

as an indication of very high temperatures, [see the unphysical temperature $T \sim 15$ MeV for beryllium in Fig. 6(b)].

Further, the mean number of heavily ionizing prongs N_h for all the stars emitting heavy fragments is ~ 19 . This also indicates excitation energies of the same order as the total binding energy.

We, therefore, conclude that the present observations emphasize the results drawn from the previous paper¹⁴ that the majority of the fragments cannot be emitted in nuclear evaporation processes.

ACKNOWLEDGMENTS

The authors are indebted to Dr. W. H. Barkas and Dr. E. J. Lofgren, Radiation Laboratory, Berkeley, for very much help in exposing the plates. We thank the Royal Norwegian Council for Scientific and Industrial Research for financial support.